Information Fusion 53 (2020) 134–144

Contents lists available at ScienceDirect

Information Fusion

journal homepage: www.elsevier.com/locate/inffus

Full Length Article

Gait-based identification for elderly users in wearable healthcare systems

Fangmin Sun[a], Weilin Zang[a], Raffaele Gravina[b], Giancarlo Fortino[b], Ye Li[a,*]

[a] Joint Engineering Research Center for Health Big Data Intelligent Analysis Technology, Shenzhen Institute of Advanced Technology, Chinese Academy of Sciences, Shenzhen, China

[b] Department of Informatics, Modeling, Electronics, and Systems, University of Calabria, Italy

ARTICLE INFO

Keywords:
Wearable healthcare system
Accelerometer sensors
Gait recognition
User identification
Score level fusion

ABSTRACT

The increasing scope of sensitive personal information that is collected and stored in wearable healthcare devices includes physical, physiological, and daily activities, which makes the security of these devices very essential. Gait-based identity recognition is an emerging technology, which is increasingly used for the access control of wearable devices, due to its outstanding performance. However, gait-based identity recognition of elderly users is more challenging than that of young adults, due to significant intra-subject gait fluctuation, which becomes more pronounced with user age. This study introduces a gait-based identity recognition method used for the access control of elderly people-centred wearable healthcare devices, which alleviates the intra-subject gait fluctuation problem and provides a significant recognition rate improvement, as compared to available methods. Firstly, a gait template synthesis method is proposed to reduce the intra-subject gait fluctuation of elderly users. Then, an arbitration-based score level fusion method is defined to improve the recognition accuracy. Finally, the proposed method feasibility is verified using a public dataset containing acceleration signals from three IMUs worn by 64 elderly users with the age range from 50 to 79 years. The experimental results obtained prove that the average recognition rate of the proposed method reaches 96.7%. This makes the proposed method quite lucrative for the robust gait-based identification of elderly users of wearable healthcare devices.

1. Introduction

Nowadays, the number of elders and empty nesters worldwide takes on a rising trend, which makes their healthcare a global challenge [1]. According to recent surveys [2,3], about 77% of persons older than 65 years suffer from various types of chronic diseases, including hypertension, hyperglycaemia, asthma, stroke, cognitive decline, etc. Accordingly, the long-term and continuous monitoring of physiological parameters of elders is indispensable for reducing the risk of their morbidity and mortality.

However, the available hospital monitoring resources are in severe shortage and fail to provide a high quality of healthcare service [4]. To provide a convenient and effective remote monitoring in mobility, the wearable healthcare system was developed [5,6]. The wearable healthcare system is a body area network supporting on-body links and links to implanted devices. This network is organized around a hub (coordinator) following a star topology [7], it is also referred to as smart body area network (SmartBAN) or wearable internet of things (Wearable IoT). Under the mandate of European Telecommunication Standards Institute (ETSI), a technical committee (TC SmartBAN) was formed in 2013. It defined multiple human monitoring application cases for SmartBAN, including sleep, fall, blood pressure fluctuation, and abnormal cardiac rhythm monitoring in [8], as well as elderly at home monitoring in [9].

A typical architecture of the elderly healthcare-targeted system is depicted in Fig. 1. It implies that older adults, who usually have chronic diseases, use their wearable healthcare devices to measure the physiological [10,11] and physical [12,13] parameters they are concerned about. For the further assessment and analysis of the results obtained, the collected data and often a high-level information obtained via multisensor fusion [14]) are then uploaded to the remote server or cloud platform.

Given the increasing scope of sensitive personal information, including the physical, physiological, and daily activities, which is stored in the wearable healthcare devices, the security of the latter is essential to avoid threatening the privacy and confidentiality of the users [15]. The imposter may attack the healthcare system and illegally get access to the sensitive information. As the cognitive and learning abilities of elders are quite limited, the most diffused authentication method, which implies the input of completely matching passwords to obtain the access authority of the device, is infeasible, as elders usually have difficulties in keeping in mind the access control passwords. Consequently, studies on comprehensive security methods that would be suitable for elderly users of wearable healthcare devices are quite topical.

* Corresponding author.
E-mail address: ye.li@siat.ac.cn (Y. Li).

https://doi.org/10.1016/j.inffus.2019.06.023
Received 12 March 2019; Received in revised form 10 June 2019; Accepted 15 June 2019
Available online 17 June 2019

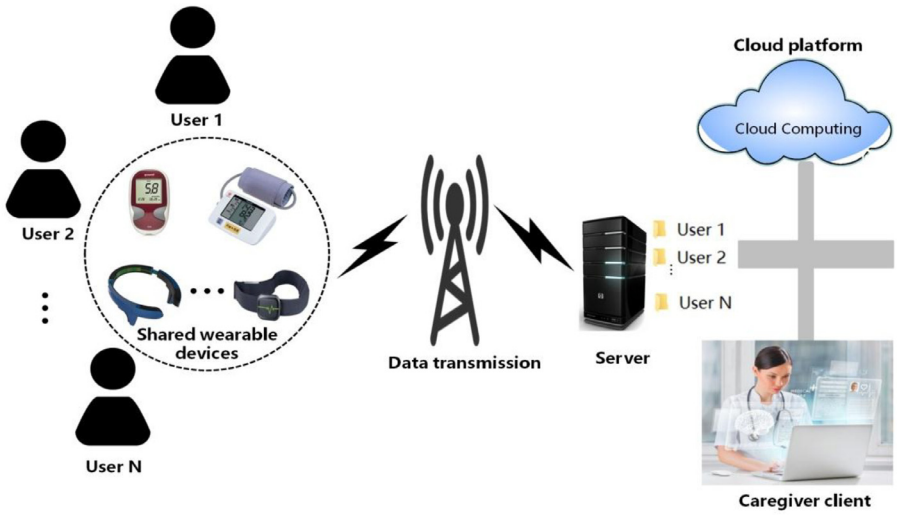

Fig. 1. Typical architecture of the wearable healthcare system.

Besides, it often becomes economically expedient to share wearable devices among family members or senior adults in the same nursing home. The users need to enter their accounts and passwords before each measurement to ensure the collected data can be uploaded to the correct user account. However, this may be problematic for elders and thus reduce the quality of experience (QoE) of wearable devices. Given this, automatic user identification seems to be the optimal solution to this problem. As seen in Fig. 1, the health monitoring devices including sphygmomanometer, blood sugar meter, electroencephalograph, heart rate band, etc., are shared by multiple users. Providing that these devices can automatically define the identity of a currently monitored person, the respective measurement data would be automatically uploaded to the appropriate account with no manual selection.

From another perspective, automatic user identification of wearable healthcare devices is vital to avoid spoofing attacks and healthcare system abuse attempts: to apply for potential health benefits that are allocated to people with certain diseases, spoofers may deliberately distribute their registered individual devices among users with such diseases and claim that the data collected from these devices are their own [16].

Studies on automatic user identification have been carried out by many researchers. Among these, camera-based face or silhouette recognition is the most popular method used for identity recognition [17-19], and it has been applied to a multitude of applications such as access control, smart security, entry and exit control, etc. However, the application bottleneck of this method lies in that the recognition performance is easily affected by illumination variation, obstacles, etc. Besides, camera-based recognition is not suitable for low-cost wearable devices, which have no cameras.

Another widespread technique is fingerprint recognition [20,21]. Fingerprint-scanning sensors (optical, capacitive, thermal, piezoresistive, and others) have been integrated into multiple off-the-shelf smart devices, such as smartphones, security doors, attendance systems, etc. However, the application of these methods requires dedicated image/fingerprint capture sensors that are rarely available in wearable devices, which limits their feasibility for the identification of wearable healthcare system users. Furthermore, the fingerprint/face recognition process needs user interaction, which may be an arduous task for elders.

Physiological signals, such as electrocardiograms and photoplethysmograms, have also been used to resolve the security issues of wearable devices in recent studies. The unique feature of the user's physiological signals makes these methods very suitable for wearable healthcare devices. An inter-pulse interval (IPI) based key generation and distribution solution for the wearable sensor networks using the electrocardiogram (ECG) signals was developed by several researcher groups [22-24]. Liu et al. proposed an ECG-based biometric human identification and authentication scheme using the multiscale autoregressive method, which made it possible to achieve high recognition rates both for the public dataset and practical test scenarios [25]. However, these methods necessitate the integration of all wearable devices with the same physiological signal sampling module, which option is not always achievable in practical applications.

Previous studies, through a large number of repeated experiments, have revealed strong similarities/dissimilarities between gaits of the same/different individuals, respectively, and proved that human gait is a unique feature that could be used for the robust identity recognition [26,27]. Moreover, as compared to the conventional biometrics like fingerprints and face recognition methods, the gait recognition method combines several advantageous features, namely high fraud-resistance, secure data collection, no need for the explicit user interaction, and continuous and long-distance authentication. This lucrative combination makes the gait a very suitable biometric parameter for user verification in wearable healthcare devices.

Gait-based biometric studies can be classified into three categories, namely machine vision-based, wearable sensor-based, and floor sensor-based ones. This study falls into the second category, and hence is focused on wearable sensor-based research results. Noteworthy is that a broader application of machine vision-based [28] and floor sensor-based approaches [29,30] is yet hindered by the lack of sophisticated specialized equipment such as high-definition cameras and pressure-sensing carpets.

There are numerous reports on gait-based biometrics. Thus, Gafurov et al. presented a gait authentication scheme based on the histogram similarity and cycle length detection methods, which was verified on 21 younger adults (20–40 years of age) [31]. Ren et al. used the gait patterns derived from acceleration readings to detect possible user spoofing in mobile healthcare systems [16]. To avoid the spoofing attacks, the user-centric and server-centric frameworks were proposed and tested using smartphone-enabled mobile healthcare systems with different locations of cell phones on the user body [16]. Alternatively, Muaaz and Mayrhofer suggested a cell phone-based gait recognition method based on the machine learning algorithms and conducted experiments, which included data on young adults [32,33]. Trung et al. analyzed the gait recognition performance using different matching methods [34]. A recent study performed by several co-authors of this paper proposed a speed adaptive gait recognition method using the individualized

threshold generated when constructing the gait template [35]. The latter method yielded high recognition rates of subjects walking at variable speeds.

However, the feasibility of major available methods of gait recognition was mainly tested on young adults, whereas their gait recognition performance for elderly subjects has yet to be validated. The intra-subject gait fluctuation for older adults is known to be more significant than that of young ones due to the natural decline in physical strength with age [36]. In contrast, the gait fluctuation of young adults is quite small since they have established their walking style; in other words, they have a stable gait pattern [37]. This makes the gait-based identity recognition of older adults a more challenging task, as compared to that of young ones, and this task is getting more urgent with the aging population global trend.

This paper proposes a gait-based identity recognition solution for the wearable healthcare system, which conveniently implements identity authentication and user recognition without user interaction. According to the recognition results, the sampled data can also be automatically uploaded to the respective folders in remote servers or cloud computing platform.

The main contributions of this study can be summarized as follows:

1. The gait template synthesis method is proposed to reduce the intra-subject gait fluctuation of elderly users. The average of several gait cycles is used to synthesize the gait template, which is more representative of a person's gait.
2. The score level fusion method for user recognition is proposed. Two matching algorithms are used to make preliminary decisions; if there are inconsistencies in the preliminary decisions, the third matching algorithm is used to provide the final decision. Such procedure is shown to improve the recognition rate of older adults.
3. The comparative analysis of gait recognition rates obtained via the cycle-based and fixed length-based gait template construction methods is performed.
4. Recognition performances are evaluated under various ground conditions and sensor placements, and the robustness of the proposed gait-based recognition method for elderly users is proved.

The rest of the paper is organized as follows. The gait characteristics and gait recognition challenges for elder users are presented in Section 2. The proposed gait-based identity recognition methods are introduced in Section 3. The experiments conducted for the verification of the proposed methods are described in Section 4, and the experimental results obtained are analyzed in Section 5. Finally, Section 6 concludes the work.

2. Challenges of gait recognition for elderly users

The deterioration of gait characteristics of elders, including the gait symmetry, balance, and consistency, implies the respective challenges related to their gait recognition.

2.1. The gait of elders has poor left-right-symmetry

Gait symmetry is an essential aspect of human walking. It is widely assumed that a healthy gait is symmetrical, while any asymmetric pattern is a sign of gait abnormality [37]. However, this assumption was not thoroughly tested, especially for elders. With age, the muscular strength/nervous system degeneration of elders results in the asymmetry of the left-right gait, which is depicted in Fig. 2. The signal was sampled from the waist centre of a male subject of 66 years of age walking on the level ground.

2.2. The gait of elders lacks consistency on time scale

Studies on the gait biometrics are based on the assumption that the intra-subject fluctuation of the gait is negligible. This assumption is valid for young adults, who have already mastered walking skills and have established their walking style but may not hold for children under ten years and elders over 50 years. The intra-subject gait fluctuation of children is relatively more extensive due to the immaturity of their walking skills, whereas that of elders increases with age, due to the natural decline of their physical strength [38]. Comparative experiments conducted in [38] revealed that the equal error rates (EER) of gait recognition for young adults (aged 20–30 years) and elderly ones (over 50 years of age) were 7 and 18%, respectively. Such a nearly 2.5-fold increase in the recognition error rate can be attributed to a poor gait consistency of elderly users.

2.3. Gait cycle periods of elders are hard to detect

Due to the left-right gait asymmetry and inconsistency on the time scale, the gait cycle periods of elders are less pronounced than those of young adults [39]. Therefore, gait recognition methods based on the gait cycle detection may be unfit for elders, and this necessitates the application of alternative methods, which would take into account the above gait-related peculiarities of elders.

3. Methodology

To resolve the problem of gait recognition of elders, a multiple matching algorithm-based method is proposed in this study, which can be reduced to the following procedures. Firstly, the Pearson correlation coefficient (PCC) and the Manhattan distance (MD) algorithms are used in parallel for the preliminary assessment of the user identity, whereas the final decision on accepting or rejecting the user identity is made via the normalization cross-correlation algorithm.

The flowchart of the above method, which includes the signal preprocessing and gait-based identity recognition procedures, is depicted in Fig. 3.

For the signal preprocessing procedure, the raw 3-axis acceleration signal is denoised by a low-pass filter. Then, the array dimensionality of the 3-axis acceleration data is reduced utilizing the principal components' analysis (PCA). At the registration phase, gait templates (T_{cycles}) are constructed by the proposed cycle-based or fixed length-based gait template construction methods. At the identification phase, the gait to be recognized (P_{cycle}) is acquired by the same methods. For the gait-based identity recognition process, the arbitration-based score level fusion algorithm is designed to improve the recognition accuracy, considering the computation complexity and the matching accuracy. The PCC and MD algorithms are first used to recognize the user's identity. If the recognition results of these two algorithms are not consistent, the additional algorithm, namely the normalization cross-correlation (NCC), is realized to make the final decision. The processing procedure is described in more detail in the following subsections.

3.1. Signal preprocessing methods

According to the signal preprocessing procedure depicted in Fig. 3, the raw acceleration signal is firstly filtered using a Butterworth low-pass filter to remove the high-frequency noise. The cut-off frequency of 3 Hz is preset, insofar as the average gait frequency is between 1.7 and 2.7 Hz. Next, the filtered signal is further processed to extract the gait template and probe data.

As mentioned in Section 2, the gait characteristics of elders, which include irregular cycles and unclear boundaries between two cycles, may result in malfunctioning/increased error rates of cycle extraction methods. To solve this problem, this study proposes a new template construction method, which does not directly use the acceleration signal to extract gait cycles. Instead, the synthesized signal is applied to construct the template. Through this method, the asymmetry inconsistency of the elderly gait can be resolved.

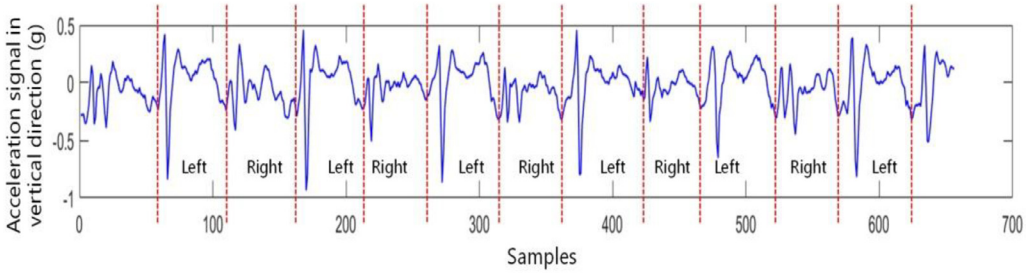

Fig. 2. The left-right-gait asymmetry of an elder male user.

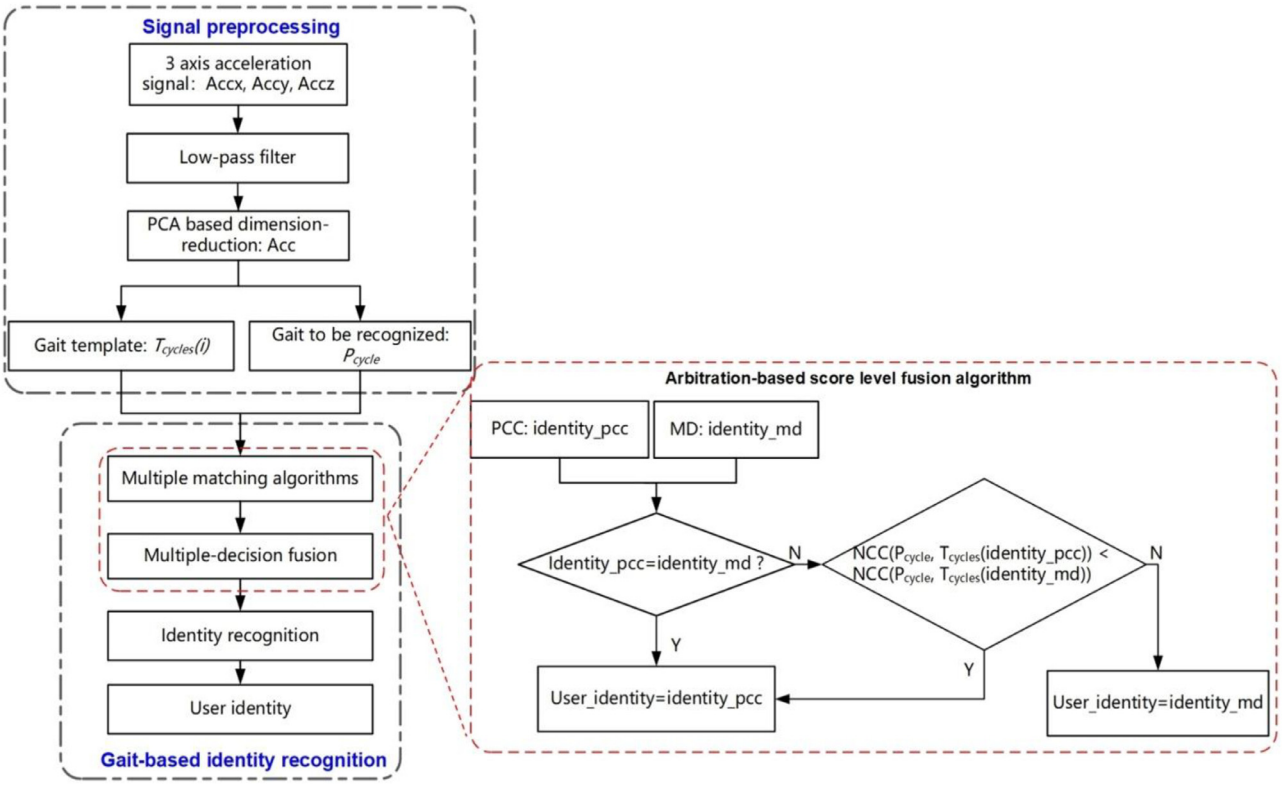

Fig. 3. The signal-processing flowchart of the proposed method.

To reduce the signal processing complexity, the 3-axis acceleration signal is firstly synthesized into unidimensional one using the principal components' analysis (PCA). This is a statistical procedure that uses an orthogonal transformation to convert a set of observations of possibly correlated variables into a set of values of linearly uncorrelated variables called principal components [40]. As the same motion source generates the acceleration signals in the three directions, they should have a strong correlation. The application of PCA for recognizing the gait via the first principal component of the 3-axis acceleration signal was found to be very effective. Algorithm 1 depicts the signal preprocessing procedure.

Algorithm 1 Signal preprocessing.

Input:
Acceleration signal: Data = $\{x_i\ y_i, z_i, i=1,2,\ldots L\}$;
Procedure:
1. $T_{data} = PCA(Data) = \{t_i\ , \%\ i=1,2,\ldots L\}$; % *dimension reduction*
Output: T_{data}

Fig. 4 depicts the 3-axis acceleration signal sampled from the centre of the user waist when the user was walking on the level ground, as well as the first principal component. The latter exhibits a more pronounced periodicity than the original signal.

3.2. Gait template construction method

The mapping signal after PCA is then processed by two different methods to construct the gait templates, namely the cycle- and fixed length-based ones. The respective procedures can be described as follows.

3.2.1. Cycle-based method

According to the cycle-based method, the signal cycles are extracted and averaged to construct the template. Firstly, the minimum points of the PCA signal are detected and selected to extract the cycles. Insofar as cycles may differ by length, the length normalization of the detected cycles should be performed using the cubic spline interpolation algorithm. Then, the cycles are summed and averaged to reduce the intra-subject fluctuation. The respective pseudo-code is presented in Algorithm 2.

An example of the extracted cycles and the constructed cycle-based gait template is illustrated by Fig. 5. The signal was also sampled from the centre of the waist while the user was walking on the level ground. In the proposed cycle-based gait template construction method, seven

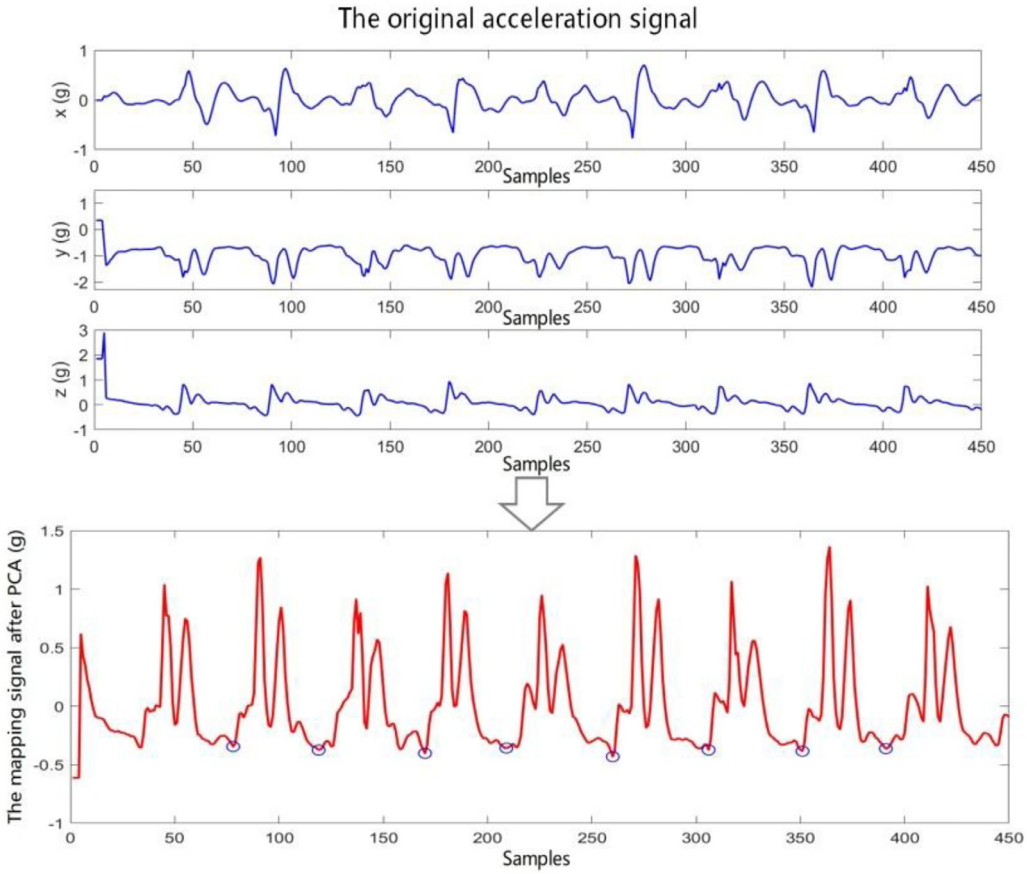

Fig. 4. Original acceleration signal and the mapping signal obtained by the dimensional reduction via PCA.

Algorithm 2 Cycle-based method.

Input:
Acceleration signal: $T_{data} = \{t_i$, % $i = 1,2,...,L\}$;
Smaple frequency: f_s;
Procedure:
1. min_index = arg min(T_{data});%find the position of the local minimum points of the Acc
2 start_p = T_{data} (min_index(1));%the start point is the first local minimum point
3. freq = fft(T_{data});%Single-Sided Amplitude Spectrum of signal
4. f_{max} = arg max(freq); % estimate the cycle frequency
5. len = f_s/f_{max};%the estimated cycle length
***6. for** i=1:1:N %extracted N cycles*
7. searchRange = [start_p + len −d, start_p + len + d];
8. end_p = the position of the local minimum point lacate in the searchRange;
9. cycle = Acc(start_p: end_p);%the extracted cycle
10.cycle= spline(cycle, 100);%normalize the length of the extracted cycle to 100 samples
11.sum_cycle = sum_cycle+cycle;
12.start_p = end_p;
13.end for
14.avg_cycle = sum_cycle/N;
Output: *avg_cycle;*

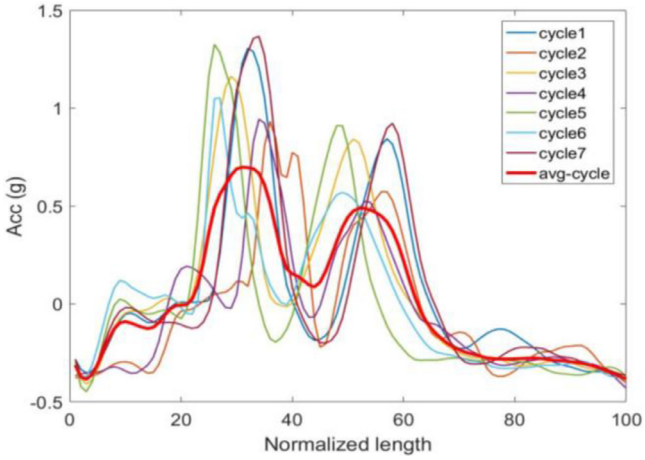

Fig. 5. The extracted gait cycles and the averaged gait cycle.

gait cycles were used to assess the average gait cycle. As the general gait frequency was about 2 Hz, the gait template construction time was approximately 3.5 s.

3.2.2. Fixed length-based method

For the fixed length-based method, a fixed length (S) of the signal was extracted to construct the template. The data at the starting and ending periods are removed to reduce the interference of the respective irregular (start and stop) user body motions. In this study, the impact of the fixed length S on the recognition rate was explored, and the optimal length value was assessed at 300. The detailed procedure of the fixed length-based method is given in Algorithm 3.

Algorithm 3 Fixed length-based method.

Input:
Acceleration signal: $T_{data} = \{ t_i$, % $i = 1,2, \ldots L\}$;
Procedure:
1. fixed_length = $\{t_j$; % $j = 100, 101,...(100+S-1)\}$;
Output: *fixed_length;*

3.2.3. Establishment of gait template

For the above two methods, the signal sampled from the authenticated users composed the template vector as follows:

$$Temps = \begin{bmatrix} Temp_1 & Temp_2 & \dots\ \dots & Temp_M \end{bmatrix} \quad (1)$$

where $Temp_i$ represents the gait template of user i, whereas M is the number of authenticated users in this system, whose gait templates compose the template vector *Temps*. For the signal used in the test, the preprocessing results for the cycle- and fixed length-based methods are stored in *Test_gait*. The latter contains only the gait signals of a single unknown subject, while *Temps* consists of the gait templates of M authenticated subjects.

According to the template construction methods, the data stored in the template vector and those used in tests have the same length. Therefore, the test gait signal length should be equal to that of the gait template.

3.3. Gait-based identity recognition methods

3.3.1. User recognition algorithm

To recognize the user's identity, the distance- or metric function-based methods are usually applied. There are many template-matching algorithms including the cross-correlation, Manhattan distance, Euclidean distance, dynamic time warping (DTW), Pearson correlation coefficient (PCC), etc. However, the above single matching algorithms have certain drawbacks. For example, DTW measures a distance-like quantity between two given sequences but does not guarantee the triangle inequality to hold. As a result, the series may get so warped that their discriminative patterns will be lost [41].

In this study, a multiple-decision method is proposed to improve the recognition performance. Firstly, two matching algorithms are run in parallel, and the decisions they make are compared. If these are different, the third matching algorithm is performed to compare the two decisions further and make the final decision. The three matching algorithms used in this study are briefly described below.

The first matching algorithm used is the Pearson correlation coefficient (PCC). It is considered to be the optimal choice for measuring the correlation between variables of interest because it is based on covariance. It provides information on the correlation, as well as the relationship trend [42]. This method is also referred to as the Pearson product moment correlation (PPMC), which shows the linear relationship between two sets of data. Its value is ranged between +1 and −1, where 1, 0, and −1 correspond to the total positive, zero, and total negative linear correlations, respectively. The PCC definition is as follows:

$$\rho_{x,y} = \frac{cov(x,y)}{\sigma_x \sigma_y} = \frac{E\left((x-\mu_x)(y-\mu_y)\right)}{\sigma_x \sigma_y}, \quad (2)$$

where *cov* is the covariance between x and y, σ_x and σ_y are the standard deviations of x and y, respectively, μ_x and μ_y are the means of x and y, respectively, while E is the expectation. Correlation between datasets is a measure of their relation closeness. The PCC between the gait cycle template and the user's gait cycles is instrumental in determining the user validity.

At the same time, another matching algorithm based on Manhattan distance (MD) is used for the first-round matching. The MD between two sequences x and y with length N can be calculated via Eq. (3)

$$md(i,j) = \sum_{i=1}^{N} |x_i - y_i| \quad (3)$$

If the recognition results obtained by the above two algorithms are different, a third matching algorithm would be used to re-judge the two different identities and make the final decision on the user identity. The algorithm used here is the normalization cross-correlation (NCC). Cross-correlation is the primary statistical approach to image registration. It is used for template matching or pattern recognition and reflects the degree of similarity between the image and template [43]. In contrast to the above two template matching algorithms, NCC exhibits higher computational complexity and more accurate matching performance.

3.3.2. Arbitration-based score level fusion algorithm

For the gait recognition process, gait samples from unknown users are used to test the recognition performance of the proposed method.

The collected data can be presented as $Data = \{x_i, y_i, z_i, i = 1, 2, \dots, L\}$, where x, y, and z represent the acceleration data in the respective three directions of the sensor, while L is the length of the collected data. Firstly, the three dimensions of the T_{data} signal are processed via the above signal-preprocessing method using PCA, and $T_{data} = t_i$, $i = 1,2,\dots, L$

Then, according to the template construction method (cycle-based or fixed length-based) used in the previous section, the gait signal used for the test is segmented into cycles or portions of fixed length. For the cycle-based method, the test signal is firstly segmented into K cycles, as shown in Eq (4):

$$Test = \left\{cycle_1, cycle_2, \dots, cycle_K\right\} \quad (4)$$

Then, the obtained cycles are averaged to get *Test_Gait* for the recognition procedure of the next step.

$$Test\_Gait = \frac{1}{K}\left(cycle_1 + cycle_2 + \dots + cycle_K\right) \quad (5)$$

For the fixed length-based method, the test signal can be expressed as:

$$Test\_Gait = t_s \ \ s = L, L+1, \dots, L+S-1 \quad (6)$$

The gait template established in the previous section has been given in Eq (1). The recognition procedure is shown in Algorithm 4, where M is the number of registered users.

Algorithm 4 Gait recognition process.

Input:
Gait templates: Temps
Gait cycle used for identification: Test_gait
Procedure:
1. ***For*** *i=1:1:M*
2. Pcc(i) = pcc(Test_gait, Temps(i));
3. Md(i) = md(Test_gait. Temps(i));
4. End for
5. [min_Pcc, min_index_Pcc]= findmin(Pcc);
6. [min_Md, min_index_Md] = findmin(Md);
7. ***If*** *min_index_Pcc = min_index_Md:;*
8. Identity_No=min_index_Pcc;%Confirm the identity of the user
9. Else
10. Ncc_Pcc=NCC(Test_gait, Temps(min_index_Pcc));
11. Ncc_Md=NCC(Test_gait, Temps(min_index_Md));
12. If *Ncc_Pcc<Ncc_Md*
13. Identity_No = min_index_Pcc;
14. Else
15. Identity_No = min_index_Md;
Output: *Identity No.*

Firstly, PCC and MD between *Test_gait* and each *Temp* gait in *Temps* are computed. Next, the locations of the maximum PCC (*max_index_pcc*) and minimum MD (*min_index_md*) are detected, which means that, according to PCC/MD values, *Test_gait* is the closest to *Temp* with subscript *max_index_pcc/min_index_md*.

If *max_index_pcc* and *min_index_md* are points of the same *Temp*, then *Test_gait* values are recognized to have the same identity as *Temp* with subscript *max_index_pcc/min_index_md*. However, if *max_index_pcc* and *min_index_md* are points of two different *Temps*, the third matching algorithm (NCC) should be applied to compare the normalized cross-correlation between the two *Temps* with the *Test_gait*, and the identity would be recognized to be the same with that *Temp*, for which the normalized cross-correlation is more significant.

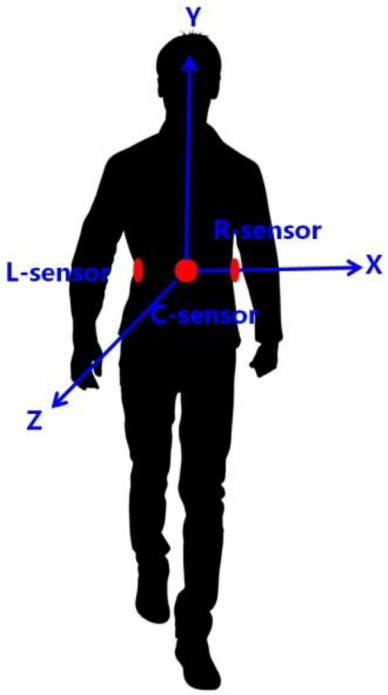

Fig. 6. Placement of the acceleration sensor nodes.

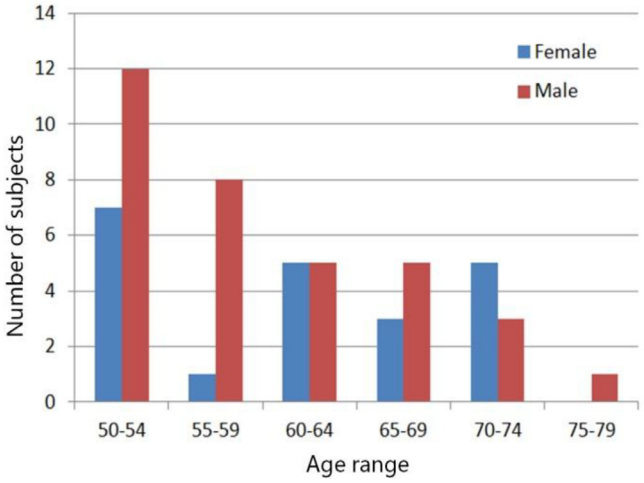

Fig. 7. Distribution by age and gender of the sub-dataset used for this study.

4. Experiments

In this section, the performance of the proposed recognition method is tested via the OU_ISIR public dataset [44]. The impact of the sensor placement in different body locations and ground conditions on the recognition performance is explored and discussed.

4.1. Data sources

The aging gait provided by OU-ISIR gait database is used to test the performance of the proposed method. There are gait samples of 744 subjects with age ranging from 2 to 78 years, including 64 older adults of age over 50 years. The accelerometer data are sampled at 100 Hz with a measuring range of ±8 g. As this study is mainly focused on gait recognition, only the gait samples of 64 older adults over 50 years are used.

The OU_ISR uses three IMUZ sensors (each one including a triaxial accelerometer). The left, right, and central IMUZ sensors (denoted as L-, C-, and R-sensor, respectively) are placed on the user's waist as shown in Fig. 6. For each subject and each sensor, two sequences for the level walk (*level walk1* and *level walk2*), one sequence for the *upslope walk*, and one sequence for the *downslope walk* were extracted. As a result, each subject had 12 traces (3 sensors × 4 traces) recorded in total [38].

The dataset has several advantages, including a large number of subjects with a balanced gender ratio, variations of sensor locations, and ground slope conditions. The gender and age distributions of the used sub-dataset are shown in Fig. 7.

4.2. Evaluation method

For the evaluation criterion, the impact of the ground condition on the recognition rate was studied for each (central, left, and right) sensor. Then, using the *level walk1* sequence sampled from central sensors to construct the template and *level walk1* sequence sampled from the left and right sensors as test samples to evaluate the impact of the sensor placement on the recognition performance.

The template for each subject was extracted from the *level walk1* sequence sampled by C-sensors, while *level walk2, upslope walk*, and *downslope walk* sequences were used as test samples to verify the recognition performance of the proposed method for different ground condition scenarios. The *level walk2* sequences sampled by C-, L-, and R-sensors were used to evaluate the impact of sensor placements on the recognition rate.

The conventional recognition performance of the method was evaluated by receiver operating characteristic (ROC) curve, which reflected a trade-off between false rejection rate (FRR) and false acceptance rate (FAR) when the threshold was changed by a receiver in personal recognition scenarios. However, in this study, the individualized threshold was automatically generated, so that FAR and FRR values were calculated and compared with the available results.

The cumulative match characteristics (CMC) curves were constructed in "rank versus identification rate" coordinates to evaluate the recognition performance for different scenarios. Each CMC curve indicated the cumulative probability of a match being within the top *n* closest matches [45].

The recognition rate of the proposed method was evaluated for different scenarios. The recognition rate was defined as the ratio of the number of accurately recognized subjects and the number of the total subjects enrolled in the tests.

5. Results and discussion

In this section, the user recognition performance of the proposed method is discussed. The effects of the sensor placement and ground conditions on the gait-based identity recognition performance were analyzed in detail.

5.1. Impact of the sensor placement on the recognition rate

To study the effect of sensor placement on the recognition rate, the left, right, and central IMUZ sensors placed on the user's waist were considered. For each sensor placement, the *level walk1* sequence was used to construct the gait template, whereas the *level walk2* sequence was applied for the performance test. The recognition performances of the cycle- and fixed length-based methods were tested. The obtained CMC curves of the three sensor placements are depicted in Fig. 8. Their comparative analysis provided the following findings.

(1) For both cycle- and fixed length-based methods, the recognition rate of the central sensors was higher than that of the left and right ones. This can be explained by the fact that sensors placed on the left and right sides of the waist are more prone to be affected by other body parts' movement, e.g., lifting arms.

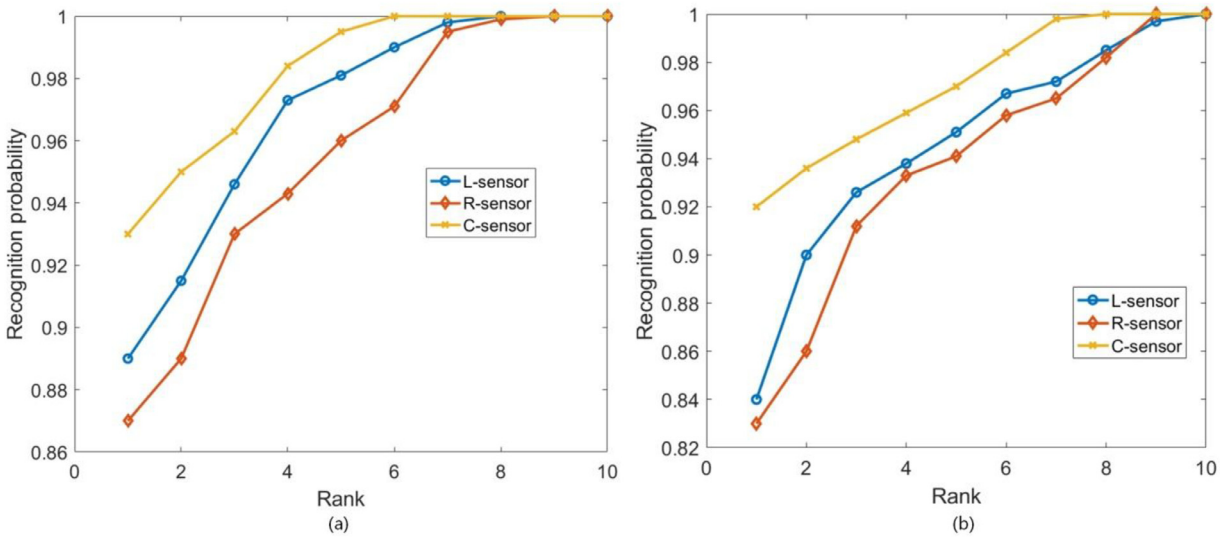

Fig. 8. The impact of sensor placements on the recognition performance (a) cycle-based method (b) fixed length-based method.

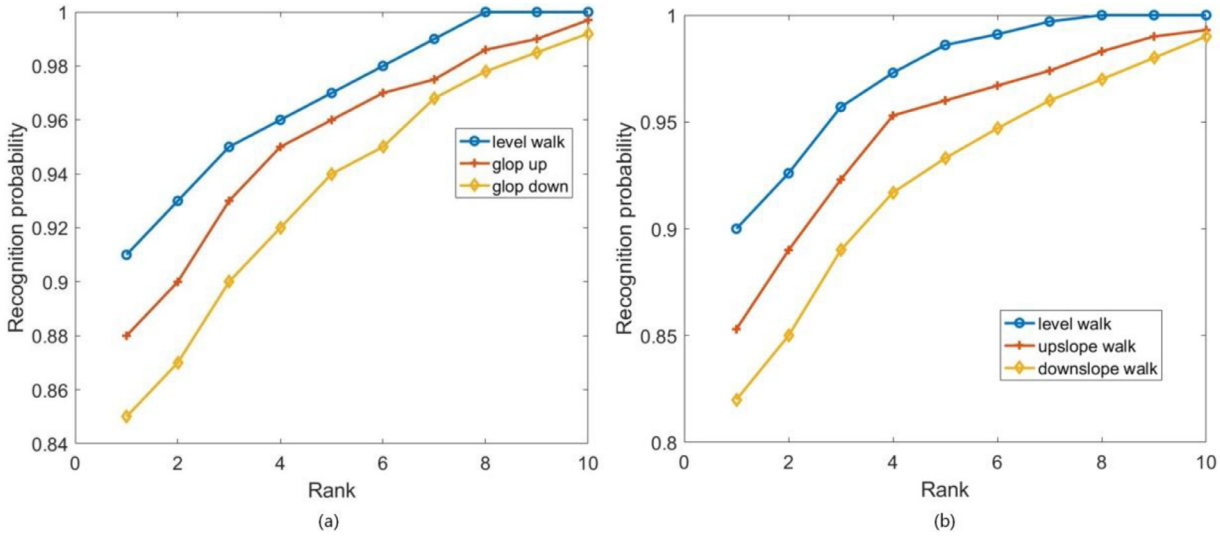

Fig. 9. The impact of ground conditions on the recognition performance (a) cycle-based method (b) fixed length-based method.

(2) The recognition rate of the cycle-based method was higher than that of the fixed length-based one. This can be attributed to the fact that the gait signal extracted by the cycle-based method contains more complete gait features than that obtained via the fixed length-based one.
(3) For all sensor placements, the rank-1 recognition probability rates of both proposed methods exceeded 0.8.

5.2. Effect of ground conditions on the recognition rate

For the performance evaluation under different ground conditions, the gait sequences sampled by the central sensors were used. For each subject, the *level walk1* sequence was adopted to construct the gait template, whereas the sequences of different ground conditions (*level walk2, upslope walk*, and *downslope walk*) were applied to evaluate the recognition rate. The performances of the cycle- and the fixed length-based methods were compared for the three ground conditions. The obtained recognition results are depicted in Fig. 9. According to the test results, the recognition rate for the level walk (flat ground) was superior to those of the upslope or downslope walks (slope ground). This trend was not unexpected: insofar as the gait template was extracted from the level walk signal, its matching rate with the test signal from the slope walk was inferior to that from the level walk. Nevertheless, for all three ground conditions, the rank-1 accuracy of the cycle- and fixed length-based methods exceeded 0.82, and the rank-1 accuracy of both methods exceeded 0.9 when users walked on the flat ground (level walk).

5.3. Performance comparison of the fusion and single methods

To validate the efficiency of the fusion matching method used for gait recognition proposed in this study, the comparative analysis of results provided by the fusion method and single matching methods (PCC, MD, and NCC) was performed. Firstly, the sequences sampled by the three sensors on the flat ground were used for each subject. The *level walk1* and *level walk2* were used as the gait template and the test sample, respectively. Secondly, the sequences sampled by the central sensors under three ground conditions were used: *level walk1* as the gait template; *level walk2, upslope walk*, and *downslope walk* sequences as test samples.

The recognition results of the single and score level fusion matching method tested on data sampled from different sensor placement are shown in Fig. 10. The test results imply that the proposed score level fusion matching method has superior recognition performance than any

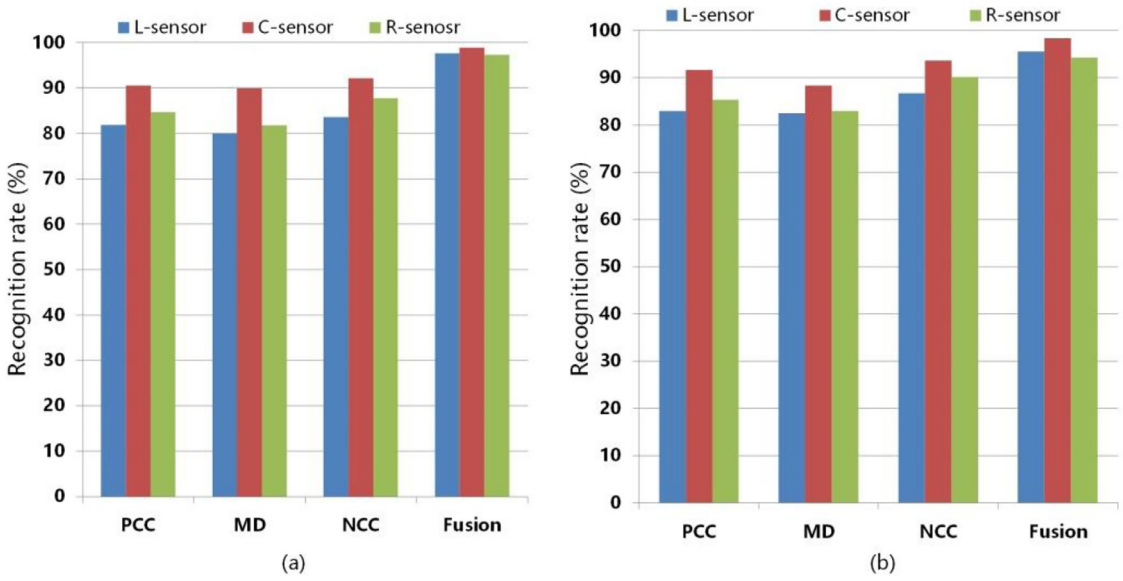

Fig. 10. The impact of the sensor placement on the recognition rate (a) cycle-based method (b) fixed length-based method.

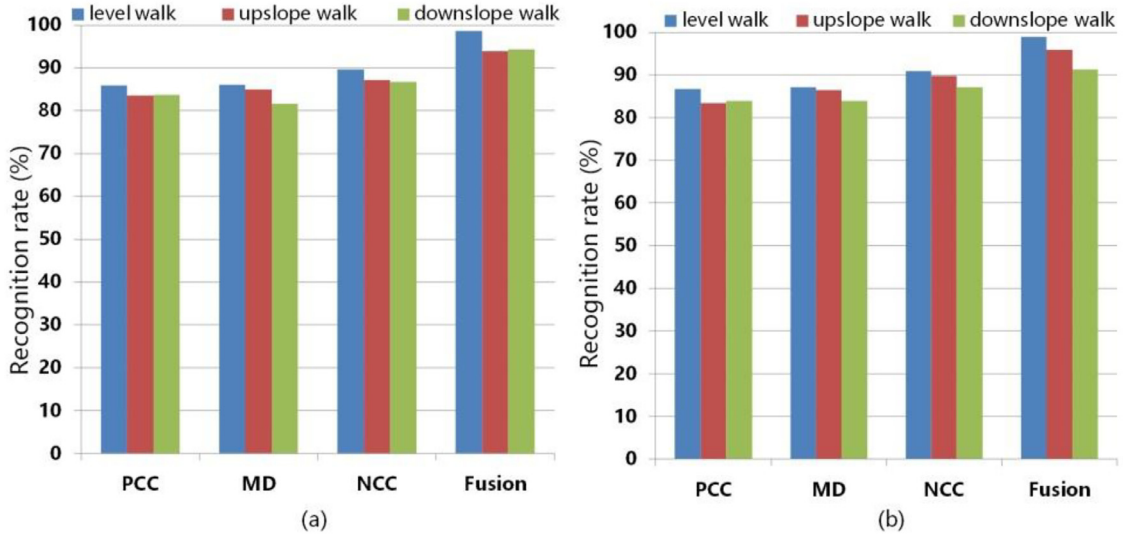

Fig. 11. The impact of ground conditions on the recognition rate (a) cycle-based method (b) fixed length-based method.

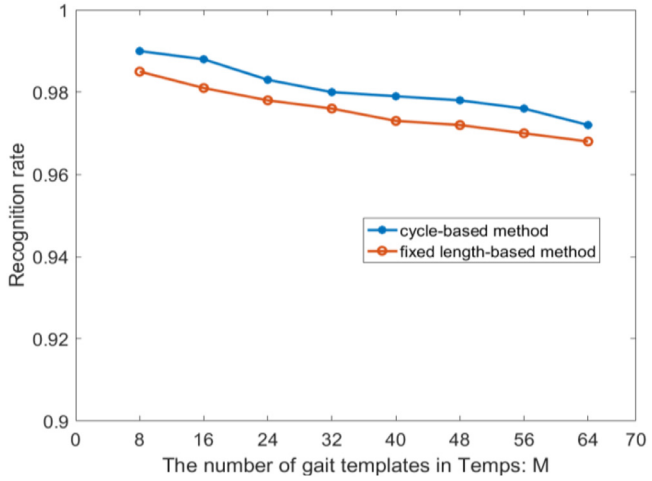

Fig. 12. The impact of the number of templates in *Temps* on the recognition rate.

of the single matching methods for all three sensor placement scenarios. Similar to the results obtained in study [35], the recognition rate of the central sensor was higher than those of the left and right ones for all matching methods used.

The test results for the comparison of the fusion and single methods under different ground conditions are shown in Fig. 11. They imply that the recognition rate of the proposed score level fusion method is superior to those of any single matching algorithms for all ground conditions, and the recognition performance of the level walk was higher than that of the upslope walk and downslope walk ground conditions.

From the test results shown in Figs. 10 and 11, one can conclude that the NCC has a better recognition performance than those of the other two matching methods. For this reason, the NCC was chosen as the final decision-making matching algorithm.

5.4. *Effect of the template size on the recognition rate*

Experiments with different number M of gait templates in $Temps = \{Temp_1, Temp_2, \ldots, Temp_M\}$ were carried out and analyzed. To avoid the

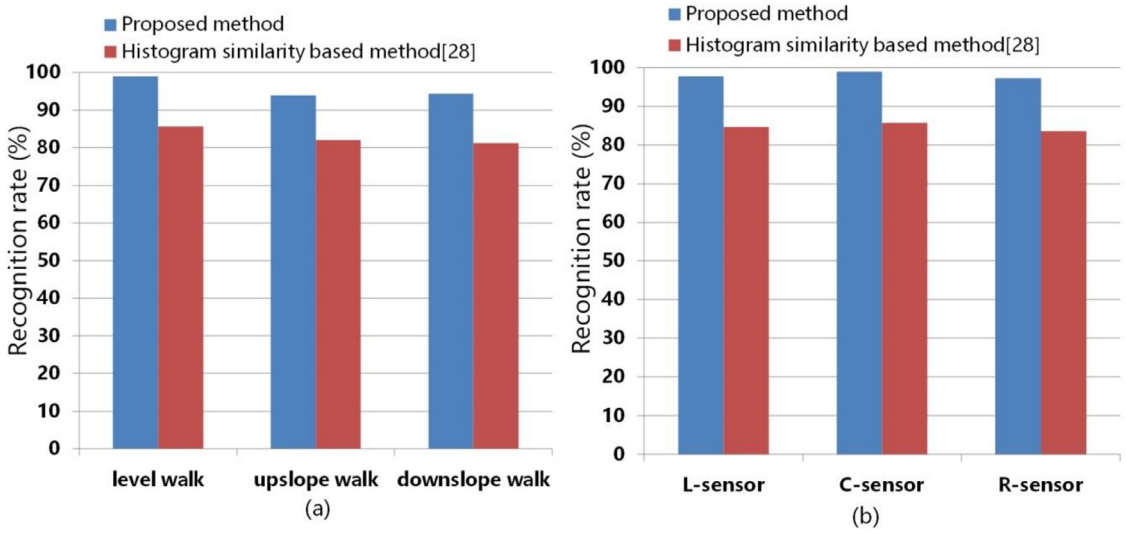

Fig. 13. Comparison of identity recognition of older adults by the proposed method and the histogram similarity based method.

influence of other factors, only the sequences sampled by the central sensors on the flat ground were used in this experiment.

The analysis of the test results depicted in Fig. 12 implies that an increase in the number of gait templates in *Temps* would slightly reduce the user recognition rate. The gait cycle (*Test_Gait*) waiting to be identified needs to be compared with all templates in *Tmeps* to finally determine the identities of the *Test_Gait,* so when the number of gait templates in *Temps* increases, more comparison operations are needed, which may lead to more matching errors and reduce the identity recognition accuracy.

5.5. Comparative analysis of recognition performance via the available method and proposed one

The proposed score level fusion scheme was applied to older adults, and its recognition performance was compared to that of the known scheme [31], which ensured the gait-based identity recognition by the histogram similarity algorithm. For comparison, only the cycle-based gait template construction method was considered in this experiment, the number of gait templates in *Temps* M was set to 64, whereas a 10-bin histogram was computed for the histogram similarity method. The identity recognition rates for different sensor placements and various ground conditions were assessed and compared.

First, using the acceleration data sampled from the centre sensors, the recognition rate of the proposed method was compared with that of the histogram similarity-based method [31] under different ground conditions. The test results as shown in Fig. 13(a) strongly indicate that the proposed score level fusion method outperforms that adopted in [31] under all ground conditions under study. This is can be attributed to the fact that the histogram similarity-based method neglects the intra-subject gait fluctuation of elderly users.

Next, the acceleration data sampled when older adults walked on the flat ground were used to compare the identity recognition rate of the two methods with three different placements of IMUZ sensors. The test results shown in Fig. 13(b) also prove the recognition rate improvement by the proposed method, as compared to that of [31], for all three sensor placements.

6. Conclusions and future work

To improve the recognition performance of wearable devices for older adults, we proposed an acceleration-based gait recognition method, which involved cycle- and fixed length-based procedures of the template construction, as well as the arbitration-based score level fusion matching technique. The proposed method was applied to a public dataset containing acceleration signals of 64 older adults of age ranging from 50 to 79 years. The experimental results showed that the recognition rate via the proposed method was improved by 26.7% on the average, as compared to available PCC-based single matching methods. The follow-up studies will address the gait recognition of children and patients with muscle and nerve diseases, whose gait patterns are unstable. Moreover, additional user identification tests of older adults will be conducted with sensors' placement in various body locations and involve different realistic scenarios to evaluate the robustness and reliability of the proposed approach. The computation and memory cost of the proposed method will be analyzed, and the relationship between the processing time and the identification accuracy will also be studied in our future work.

Acknowledgment

This study was sponsored by the National Natural Science Foundation of China (grant numbers 61702497 and U1801261), the Shenzhen Science and Technology Projects (grant numbers JCYJ20170412110753954 and JCYJ20170413161515911), the Special Fund Project for Overseas High-Level Innovation and Entrepreneurship Talents (grant number KQJSCX20170731165939298), Special Support Plan for Technological Innovation Leading Talents of Guangdong Province of China (grant number 2014TX01X060), and Major Projects of Guangdong Province of China (grant numbers 2017B030308007 and 2015B010129012).

References

[1] M. Chand, R.L. Tung, The aging of the world's population and its effects on global business, Acad. Manag. Perspect 28 (4) (2014) 409–429 10.5465/amp.2012.0070.
[2] J.E. Crews, C.F. Chou, S Sekar, J.B. Saaddine, The prevalence of chronic conditions and poor health among people with and without vision impairment, aged ≥65 years, 2010-2014, Acad. Manag. Perspect 182 (1) (2017) 18–30, doi:10.1016/jajo.2017.06.038.
[3] S. Stewart, K. MacIntyre, S. Capewell, J.J.V. McMurray, Heart failure and the aging population: an increasing burden in the 21st century? Heart 89 (1) (2003) 49–53, doi:10.1136/heart.89.1.49.
[4] E. Kanasi, S. Ayilavarapu, J. Jones, The aging population: demographics and the biology of aging, Periodontol. 2000 72 (1) (2016) 13–18, doi:10.1111/prd.12126.
[5] G. Fortino, R. Giannantonio, R. Gravina, P. Kuryloski, R. Jafari, Enabling effective programming and flexible management of efficient body sensor

network applications, IEEE T. Hum.-Mach. Syst. 43 (1) (2013) 115–133, doi:10.1109/TSMCC.2012.2215852.
[6] M. Nazari, S.M. Sakhaei, Variational mode extraction: a new efficient method to derive respiratory signals from ECG, IEEE J. Biomed. Health Inform 22 (4) (2018) 1059–1067, doi:10.1109/JBHI.2017.2734074.
[7] Smart Body Area Networks (SmartBAN); system Description. ETSI TR 103 394 V1.1.1, Jan. 2018. https://www.etsi.org/deliver/etsi_tr/103300_103399/103394/01.01.01_60/tr_103394v010101p.pdf.
[8] Smart Body Area Networks (SmartBAN); Service and Application Standardized Enablers and Interfaces, APIs and infrastructure for interoperability management. ETSI TS 103 327 V1.1.1, Apr. 2019. https://www.etsi.org/deliver/etsi_ts/103300_103399/103327/01.01.01_60/ts_103327v010101p.pdf.
[9] H. Viittala, L. Mucchi, M. Hämäläinen, T. Paso, ETSI SmartBAN system performance and coexistence verification for healthcare, IEEE Access 5 (2017) 8175–8182, doi:10.1109/ACCESS.2017.2697502.
[10] A.H. Sodhro, A. Sangaiah, G.H. Sodhro, S. Lohano, S. Pirbhulal, An energy-efficient algorithm for wearable electrocardiogram signal processing in ubiquitous healthcare applications, Sensors 18 (3) (2018) 923, doi:10.3390/s18030923.
[11] A.H. Sodhro, S. Pirbhulal, M. Qaraqe, S. Lohano, G.H. Sodhro, N.U.R. Junejo, and Z. Luo, Power control algorithms for media transmission in remote healthcare systems, IEEE Access, 6(2018), 42384–42393. doi:10.1109/ACCESS.2018.2859205.
[12] P. Pace, G. Aloi, R. Gravina, G. Caliciuri, G. Fortino, A. Liotta, An edge-based architecture to support efficient applications for healthcare industry 4.0, IEEE Trans. Ind. Inform. 15 (1) (2019) 481–489, doi:10.1109/TII.2018.2843169.
[13] H. Ghasemzadeh, P. Panuccio, S. Trovato, G. Fortino, R. Jafari, Power-aware activity monitoring using distributed wearable sensors, IEEE T. Hum.-Mach. Syst. 44 (4) (2014) 537–544, doi:10.1109/THMS.2014.2320277.
[14] R. Gravina, P. Alinia, H. Ghasemzadeh, and G. Fortino, Multi-sensor fusion in body sensor networks: state-of-the-art and research challenges, Inf. Fusion, 35(2017), 68–80. doi:10.1016/j.inffus.2016.09.005.
[15] J. Merilahti, P. Viramo, I. Korhonen, Wearable monitoring of physical functioning and disability changes, circadian rhythms and sleep patterns in nursing home residents, IEEE J. Biomed. Health Inform 20 (3) (2016) 856–864, doi:10.1109/JBHI.2015.2420680.
[16] Y.Z. Ren, Y.Y. Chen, M.C. Chuah, J.E. Yang, User verification leveraging gait recognition for smartphone-enabled mobile healthcare systems, IEEE. Trans. Mob. Comput. 14 (9) (2015) 1961–1974, doi:10.1109/TMC.2014.2365185.
[17] S. Huang, A. Elgammal, J.W. Lu, Cross-speed gait recognition using speed-invariant gait templates and globality–locality preserving projections, IEEE Trans. Inf. Forensic Secur. 10 (10) (2015) 2071–2083, doi:10.1109/TIFS.2015.2445315.
[18] E. Dolatabadi, T. Babak, A. Mihailidis, An automated classification of pathological gait using unobtrusive sensing technology, IEEE Trans. Neural Syst. Rehabil. Eng. 25 (12) (2017) 2336–2346, doi:10.1109/TNSRE.2017.2736939.
[19] X. Chen, J. Weng, W. Lu, J.M. Xu, Multi-gait recognition based on attribute discovery, IEEE Trans. Pattern Anal. Mach. Intell. 40 (7) (2017) 1697–1710, doi:10.1109/TPAMI.2017.2726061.
[20] K. Cao, A.K. Jain, Automated latent fingerprint recognition, IEEE Trans. Pattern Anal. Mach. Intell. 41 (4) (2018) 788–800, doi:10.1109/TPAMI.2018.2818162.
[21] A. Wagner, J. Wright, A. Ganesh, Toward a practical face recognition system: robust alignment and illumination by sparse representation, IEEE Trans. Pattern Anal. Mach. Intell 34 (2) (2012) 372–386, doi:10.1109/TPAMI.2011.112.
[22] F. Miao, S.D. Bao, Y. Li, Biometric key distribution solution with energy distribution information of physiological signals for body sensor network security, IET Inf. Secur. 7 (2) (2013) 87–96, doi:10.1049/iet-ifs.2012.0104.
[23] S. Pirbhulal, H. Zhang, W. Wu, S.C. Mukhopadhyay, Y.T. Zhang, Heartbeats based biometric random binary sequences generation to secure wireless body sensor networks, IEEE Trans. Biomed. Eng. 65 (12) (2018) 2751–2759, doi:10.1109/TBME.2018.2815155.
[24] W. Wu, S. Pirbhulal, G. Li, Adaptive computing-based biometric security for intelligent medical applications, Neural Comput. Appl. 1-10 (2018), doi:10.1007/s00521-018-3855-9.
[25] J. Liu, L. Yin, C. He, B. Wen, X. Hong, and Y. Li, A multiscale autoregressive model-based electrocardiogram identification method, IEEE Access, 6(2018), 18251–18263. doi:10.1109/ACCESS.2018.2820684.
[26] S. Sprager, M.B. Juric, Inertial sensor-based gait recognition: a review, Sensors 15 (9) (2015) 22089–22127, doi:10.3390/s150922089.
[27] N.M. Bora, G.V. Molke, H.R. Munot, Understanding human gait: a survey of traits for biometrics and biomedical applications, in: IEEE Int. Conf. Energy Syst. & App., 2015, pp. 723–728, doi:10.1109/ICESA.2015.7503444.
[28] A. Mosenia, S. Sur-Kolay, A. Raghunathan, N.K. Jha, CABA: continuous authentication based on Bioaura, IEEE Trans. Comput. 66 (5) (2017) 759–772, doi:10.1109/TC.2016.2622262.
[29] H. Ma, W.H. Liao, Human gait modeling and analysis using a semi-Markov process with ground reaction forces, IEEE Trans. Neural Syst. Rehabil. Eng. 25 (6) (2017) 597–607, doi:10.1109/TNSRE.2016.2584923.
[30] S. Pirttikangas, J. Suutala, J. Riekki, J. Roning, Footstep identification from pressure signals using hidden Markov models, in: Proc. Finnish Signal Processing Symposium (FINSIG'03), 2013, pp. 124–128.
[31] D. Gafurov, K. Helkala, T. Søndrol, Biometric gait authentication using accelerometer sensor, J. Comput 1 (7) (2006) 51–59, doi:10.4304/jcp.1.7.51-59.
[32] M. Muaaz, R. Mayrhofer, An analysis of different approaches to gait recognition using cell phone based accelerometers, in: ACM Proc. 11th Int. Conf. Advances in Mobile Computing & Multimedia, 2013 293–293, doi:10.1145/2536853.2536895.
[33] M. Muaaz, R. Mayrhofer, Orientation-independent cell phone based gait authentication, in: ACM Proc. 12th Int. Conf. Advances in Mobile Computing & Multimedia, 2014, pp. 161–164, doi:10.1145/2684103.2684152.
[34] T.T. Ngo, Makihara Y, H. Nagahara, Performance evaluation of gait recognition using the largest inertial sensor-based gait database, in: Proc. 5th IEEE IAPR Int. Conf. on Biometrics (ICB), 2012, pp. 360–366, doi:10.1109/ICB.2012.6199833.
[35] F. Sun, C. Mao, X. Fan, Y. Li, Accelerometer-based speed-adaptive gait authentication method for wearable IoT devices, IEEE Internet Things J 6 (1) (2018) 820–830, doi:10.1109/JIOT.2018.2860592.
[36] T. Ito, S. Umise, H. Hoshi, M. Suzuki, S. Tani, Gait measurement and evaluation system for diagnosis of elderly people's gait condition to prevent fall, in: IEEE Int. Conf. Advanced Intelligent Mechatronics (AIM), 2015, pp. 687–693, doi:10.1109/AIM.2015.7222617.
[37] R. Thorsten and F. Proessl, Effects of muscle function and limb loading asymmetries on gait and balance in people with multiple sclerosis, Front. Physiol. 9(2018), 531–531. doi:10.3389/fphys.2018.00531.
[38] T.T. Ngo, Y. Makihara, H. Nagahara, The largest inertial sensor-based gait database and performance evaluation of gait-based personal authentication, Pattern Recognit. 47 (1) (2014) 228–237, doi:10.1016/j.patcog.2013.06.028.
[39] J. Hendrickson, K.K. Patterson, E.L. Inness, Relationship between asymmetry of quiet standing balance control and walking post-stroke, Gait Posture 39 (1) (2014) 177–181, doi:10.1016/j.gaitpost.2013.06.022.
[40] E.C. Brenneman, M.R. Maly, Identifying changes in gait waveforms following a strengthening intervention for women with knee osteoarthritis using principal components analysis, Gait Posture 59 (1) (2018) 286–291, doi:10.1016/j.gaitpost.2017.07.006.
[41] G. Gafurov, E. Snekkenes, P. Bours, Spoof attacks on gait authentication system, IEEE Trans. Inf. Forensic Secur. 2 (3) (2007) 491–502, doi:10.1109/TIFS.2007.902030.
[42] P. Sedgwick, Pearson's correlation coefficient, Br. Med. J. 2012 (345) (2012) 1–2, doi:10.1136/bmj.e4483.
[43] K. Briechle, U.D. Hanebeck, Template matching using fast normalized cross correlation, optical pattern recognition XII, Int. Soc. Opt. Photon. 4387 (1) (2001) 95–103, doi:10.1117/12.421129.
[44] OU-ISIR Biometric Database. http://www.am.sanken.osaka-u.ac.jp/BiometricDB/InertialGait.html.
[45] Y.T. Zhang, G. Pan, K.I. Jia, Accelerometer-based gait recognition by sparse representation of signature points with clusters, IEEE T. Cybern. 45 (9) (2015) 1864–1875, doi:10.1109/TCYB.2014.2361287.